Half-Mode SIW Variable PIN Diode Attenuator

Gabriela Luciani, Jens Bornemann
Dept. of Electrical and Computer Engineering, University of Victoria, Victoria, BC, V8W 2Y2, Canada
gluciani@uvic.ca

***Abstract*— A half-mode substrate integrated waveguide (HMSIW) variable attenuator for operation in the 6 GHz to 10 GHz frequency range is presented. Different levels of attenuation are achieved by adjusting the level of the dc bias applied to four surface mounted PIN diodes. After fine adjustment of the PIN diode's equivalent circuit, the simulation and measured results are in good agreement, and the initial goal of up to 6 dB attenuation is achieved and verified by measurements of a prototype circuit.**

***Index Terms*—HMSIW, PIN diode, variable attenuator.**

I. INTRODUCTION

Substrate Integrated Waveguide (SIW) technology has been demonstrated to be a good compromise between conventional rectangular waveguide (RWG) and microstrip (MS). Besides presenting a reasonable result in terms of loss and Q-factor, SIW components are light, easy to fabricate, present a low-cost profile and allow the entire system to be fabricated in planar form, including planar circuitry, transitions, active components and antennas [1-3]. However, the SIW foot print can be too large for some practical circuits, affecting the integration [4]. In order to overcome this disadvantage, a novel guided wave structure derived from SIW components, the half-mode substrate integrated waveguide (HMSIW), has been proposed [4, 5]. In the HMSIW, both the waveguide width and the surface area of the metallic sheets are reduced by nearly half when compared with regular SIW technology. Moreover, the fabrication simplicity is maintained at the same level as for the SIW [6]. This design adapts the advantages of SIWs such as low profile, low transmission coefficient and low interference, but the resulting structure becomes smaller in size [7].

For manipulating large signals, attenuators are good candidates since they offer a lower power consumption (DC power consumption as low as 2mW) [8]. In [9], resistive, non-variable attenuators are proposed, where, when different surface-mount (SMT) passive resistors are applied to a HMSIW structure, a specified level of attenuation can be achieved. Variable attenuators are widely used in the radio frequency (RF) and microwave field to control power transmission, due to the necessity of reducing the signal level in order to improve the amplifier's stability [10, 11]. They have applications in modulators, automatic gain control (AGC) and radar systems [11]. PIN diodes have been used as control elements in variable attenuators due to their functionality as a variable resistance when used at high frequencies [11]. By using PIN diodes as the control element, a single structure can present different levels of attenuation.

In order to explore some of the applications of HMSIW and to demonstrate the integration of SMT components, a variable HMSIW attenuator is designed. An operating frequency range between 6 GHz and 10 GHz is selected due to the availability of PIN diodes that can be manually soldered without the need for a reflow solder process. Four PIN diodes are added to a HMSIW circuit to develop a variable attenuator with an attenuation goal of up to 6 dB, corresponding to one quarter of the power. By adjusting the level of the dc bias applied to the diodes, different levels of attenuation can be achieved as required, for instance, in an AGC environment.

II. DESIGN

A. HMSIW Design

The HMSIW is derived from an initial SIW where, by cutting the SIW (and its equivalent rectangular waveguide) in half on the vertical center plane along the propagation direction, each half of the SIW becomes a HMSIW structure [4-6]. The HMSIW design is performed using RT/Duroid 6002 substrate with $\varepsilon_r = 2.94$, $\tan\delta = 0.0012$, substrate height $h = 0.508$ mm, metal thickness $t = 17.5$ μm and conductivity $\sigma = 5.8\text{x}10^7$ S/m. The SIW design is carried out following equations presented in [12], arriving at a via hole diameter $d = 0.70$ mm, via hole distance (pitch) $p = 1$ mm, equivalent waveguide width $a_{equ} = 17.88$ mm and the actual SIW width $a = 18.43$ mm.

Since SIW and HMSIW technologies have to interface with other planar transmission lines [2, 13], the transition between SIW and MS follows guidelines in [14] to arrive at the dimensions of the transition from SIW to MS, which includes a taper and a regular section of MS. The MS line is calculated to present a 50 Ω characteristic impedance for the substrate and copper thicknesses used. The initial transition between MS and SIW involves dimensional parameters of $w = 4.60$ mm, $w_0 = 1.25$ mm and $l = 7.45$ mm according to [14].

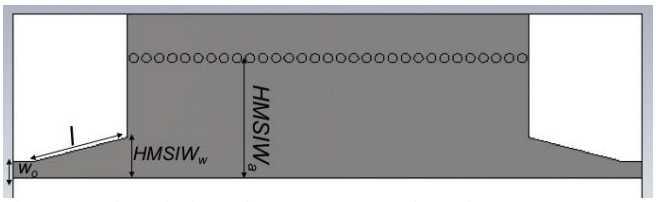

Fig. 1 Top view of microstrip-to-HMSIW-to-microstrip structure.

To arrive at the final HMSIW structure, the MS-SIW-MS is cut in half and the MS line is adapted in the remaining taper to provide a 50 Ohm characteristic impedance. The final structure is shown in Fig. 1 with the following dimensions:

$HMSIW_a$ = 9.21 mm, $HMSIW_w$ = 3.12 mm, w_o =1.25 mm and the length of the HMSIW section l =7.5 mm.

B. PIN Diode Attenuator

In order to integrate the PIN diodes into the HSMIW, a metal strip is added to form the structure at which the DC bias is applied and that will forward bias the diodes. Since the design requires a spacing of $\lambda_g/4$ between the diodes, the dimensions of the metal strip are chosen accordingly to fit four PIN diodes. The width of the slot which separates each diode from the HMSIW is optimized. Also, in order to block any RF interference from the power supply, a decoupling capacitor of 100 pF is added in parallel with the biasing plates. Thus, a smaller metal strip is added and grounded with three via roles. Table 1 presents the structural parameters for both metal strips that are added to the structure after optimization. The final structure with metal strips is shown in Fig. 2.

TABLE 1. BIASING METAL STRIP STRUCTURAL PARAMETER DIMENSIONS FOR HMSIW PIN DIODE ATTENUATOR

Structural Parameter	Dimensions (mm)
M_{w1}	4.50
M_{l1}	24.40
c	0.40
$slot$	5.80
gap_1	0.50
M_{w2}	2.00
M_{l2}	4.00
gap_2	1.97

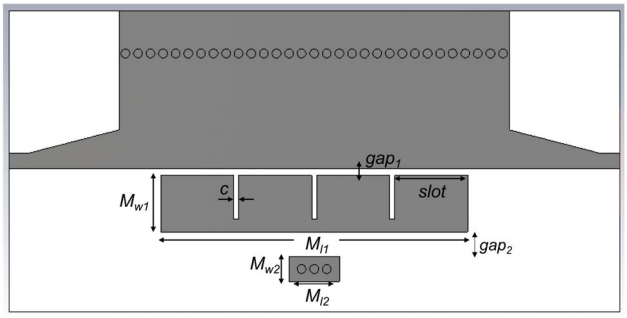

Fig. 2 Top view of the HMSIW structure with biasing metal strip.

Several attempts of PIN diode modeling can be found in the literature, e.g. [15, 16]. However, it is difficult to achieve an accurate model of this semiconductor, especially in the transient region of the device [17], which is particularly important in attenuator applications. According to [17], it is more convenient to extract the design parameters from experimental data and tune the design parameter simulation by comparison with experimental data. In addition, the PIN diode manufacturer provides the package inductance and series capacitance. However, these values change during assembly as a result of the soldering process which may affect the RF performance due to its parasitic effects [18]. Since at high frequencies, the PIN diode under forward bias appears essentially as a pure linear resistor whose value can be controlled by the DC bias [19, 20], the design process simulates the diode as an equivalent circuit with an ideal resistance. The fine adjustment of the PIN diode equivalent circuit simulation is shown in the results (Section III).

The attenuator is designed using the commercially available field solver software Computer Simulation Technology (CST). Fig. 3 shows the structure with four PIN diodes separated by a distance of 6.2 mm. The equivalent circuit is added to the design by using the lumped elements available in CST 3D EM Design. The attenuation of the design is simulated by decreasing the value of the ideal resistance until it achieves the attenuation which was initially proposed while maintaining a reflection coefficient better than -10 dB over the entire frequency range.

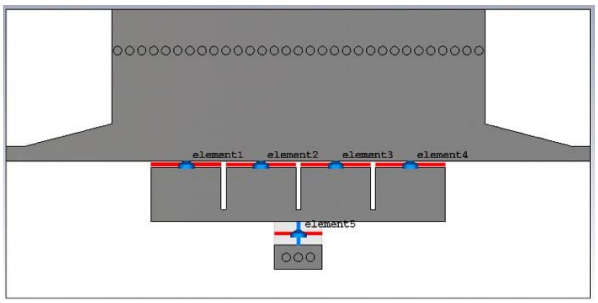

Fig. 3 Final HMSIW PIN diode variable attenuator with four PIN diodes and a decoupling capacitor added to the structure.

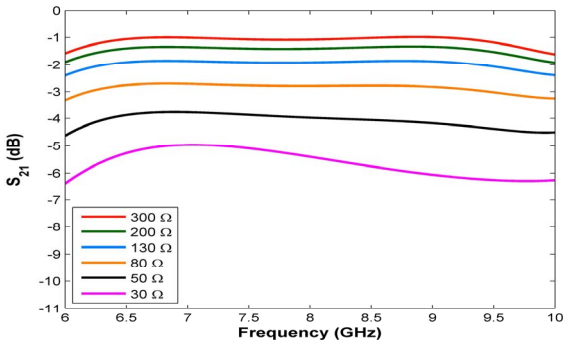

(a)

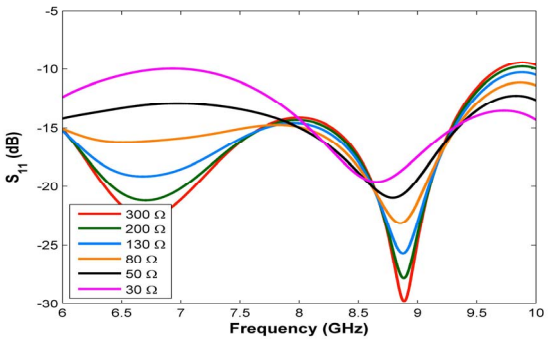

(b)

Fig. 4 Simulation of X-band HMSIW PIN diode attenuator with the attenuation level for each value of equivalent resistance; (a) transmission, (b) reflection coefficient.

Fig. 4(a) shows the attenuation level for each value of ideal resistance for the entire band. It can be seen that an

overall attenuation level of about 6 dB is achieved and that the reflection coefficient is below or close to -10 dB over the entire frequency band as shown in Fig. 4(b).

III. Experimental Characterization and Results

The HMSIW variable PIN diode attenuator is fabricated and measured for verification of the design procedure. Fig. 5 shows the final fabricated component with four PIN diodes and the biasing circuit added. The diodes used for this design are SMP1352-079Ls. A 100 pF capacitor is inserted between the bias plate and ground to block any AC interference from the power supply. A 100 Ω resistor in series with the power supply allows monitoring the current that is being applied to the diodes at each voltage bias. Measurements are performed using an Anritsu 37397C Vector Network Analyzer, an Anritsu SC5226 Test Fixture, a power supply as well as customized TRL calibration standards to deembed the coaxial-to-MS-to-HMSIW transitions.

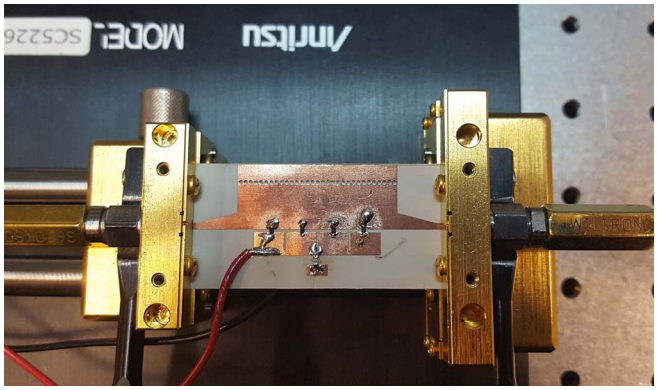

Fig. 5 Top view of the fabricated HMSIW variable attenuator with the four PIN diodes and capacitor added to the structure.

To verify the attenuator's performance, the measured and simulated results are compared. Due to the differences in the assembly of the PIN diodes when comparing with simulations, a fine adjustment in the simulation of the PIN diode's equivalent circuit is required to obtain a fair comparison between simulated and measured results. This fine adjustment is performed empirically by first adjusting the value of C_p and then the value of L_s starting with the values presented in the data sheet given by the manufacturer, C_p = 0.16 *p*F and L_s = 0.46 *n*H as shown in Fig. 6. Also, by looking at the datasheet, the manufacturer provides a table with values of R_s for each bias condition applied to the PIN diode. However, since the value presented in the data sheet is for operation at 100 MHz, R_s is adjusted to match each bias condition applied in the measurement.

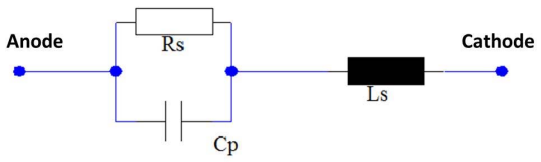

Fig. 6 Equivalent circuit of the PIN diode.

For the PIN diode's off-state equivalent circuit, the measurement is performed with a 0 mA bias current applied to the four PIN diodes. The simulation uses R_s=1000 Ω in the equivalent circuit. Fig. 7 shows the comparison of simulated versus measured results. The results present a good agreement for the PIN diode's off state, where the measured reflection coefficient is better than -10 dB from 6 GHz to 10 GHz. The measurement of the HMSIW attenuator with PIN diodes in the off state shows a maximum of -0.5 dB and a minimum of -1.5 dB transmission coefficient while the simulation predicts a maximum of -0.7 dB and a minimum of -2.2 dB. Note that the measured results have not been smoothened which explains the slight ripple in the traces.

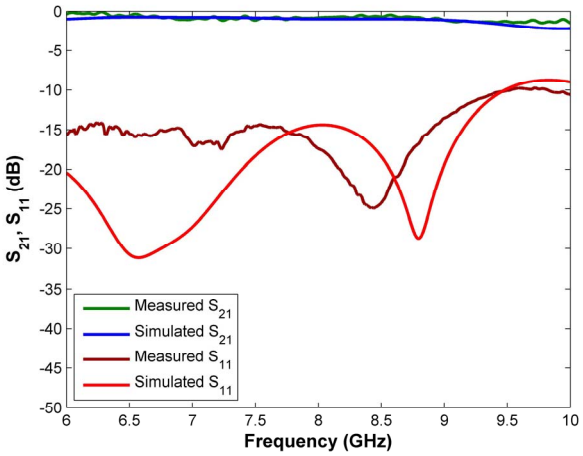

Fig. 7 S-parameter comparison between experimental and simulated results for R_s=1000 Ω and zero forward current.

Fig. 8 compares simulated versus measured results for R_s =500 Ω in the equivalent circuit and a biasing current of 5 µA applied to each diode during the measurements. The simulated and measured results show good agreement, where the measured reflection coefficient is better than -10 dB from 6 GHz to 10 GHz. The measurement presents a maximum of -0.9 dB and a minimum of -2.8 dB transmission coefficient while the simulation predicts a maximum of -1.2 dB and a minimum of -3.2 dB.

Fig. 9 depicts the comparison between simulated and measured results for R_s =200 Ω in the equivalent circuit and a biasing current of 20 µA applied to each diode in the measurements. The simulation and measured results agree very well, where the measurements present a maximum of -2.5 dB and a minimum of -5.2 dB transmission coefficient while the simulation shows a maximum of -2.4 dB and a minimum of -6.1 dB. The measured reflection coefficient is better than -10 dB from 6 GHz to 10 GHz.

Fig. 10 shows the comparison of simulated versus measured results when using R_s =150 Ω in the equivalent circuit and a biasing current of 30 µA applied to each diode during the measurements. The simulated and measured results are in good agreement, where the measurement presents a maximum of -3.5 dB and a minimum of -6.3 dB transmission coefficient while the simulation predicts a

maximum of -3.0 dB and a minimum of -7.5 dB. The measured reflection coefficient is better than -10 dB from 6 GHz to 10 GHz.

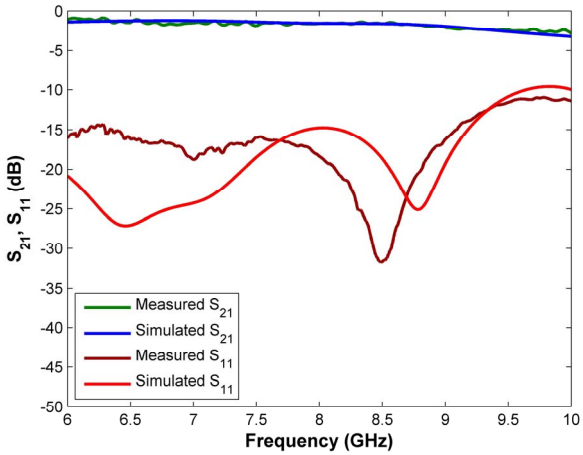

Fig. 8 S-parameter comparison between experimental and simulated results for R_s =500 Ω and a forward current of 5 µA.

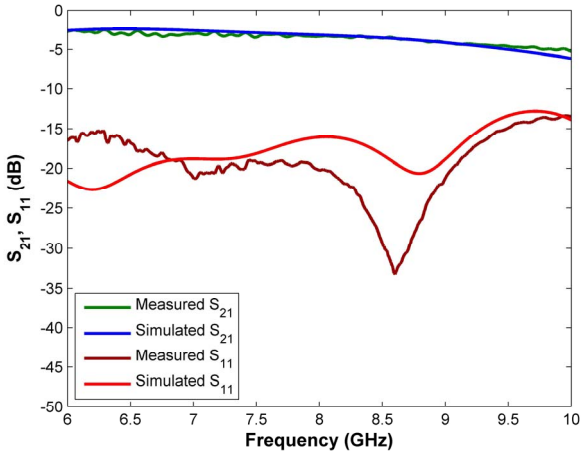

Fig. 9 S-parameter comparison between experimental and simulated results for R_s =200 Ω, forward current =20 µA.

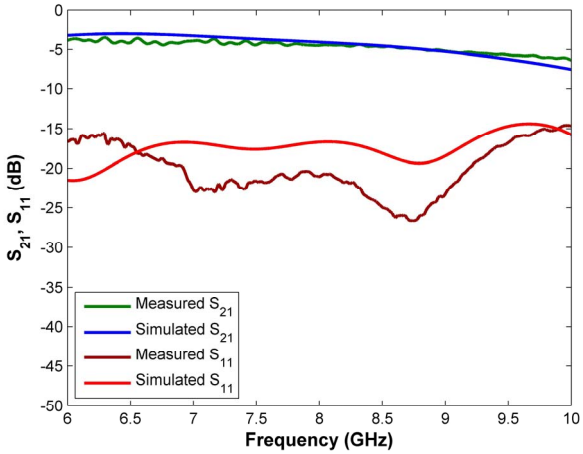

Fig. 10 S-parameter comparison between experimental and simulated results for R_s =150 Ω, forward current =30 µA.

Fig. 11 shows the comparison of simulated versus measured results for R_s =75 Ω in the equivalent circuit and a biasing current of 50 µA applied to each diode during the measurement. The simulated and measured results are in good agreement. The measurement presents a maximum of -5.4 dB and a minimum of -7.3 dB transmission coefficient while the simulation shows a maximum of -5.2 dB and a minimum of -11.5 dB. The measured reflection coefficient is better than -10 dB from 6 GHz to 10 GHz.

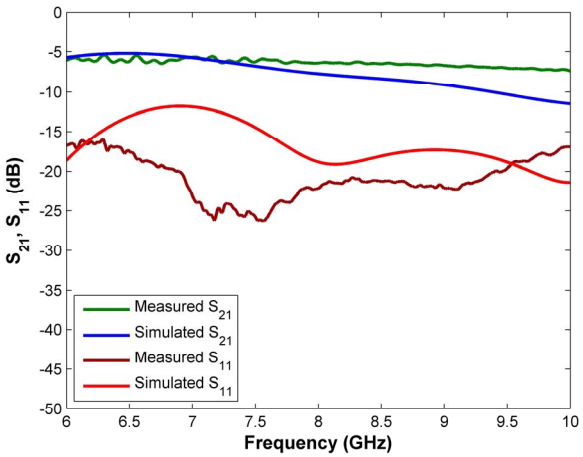

Fig. 11 S-parameter comparison between experimental and simulated results for R_s =75 Ω, forward current =50 µA.

Fig. 12 compares simulated and measured results using R_s =55 Ω in the equivalent circuit and a biasing current of 70 µA applied to each PIN diode during the measurements. The simulated and measured results agree reasonably well, and the measurement shows a maximum of -7.1 dB and a minimum of -8.3 dB transmission coefficient while the simulation predicts a maximum of -6.5 dB and a minimum of -12.5 dB. A measured reflection coefficient better than -10 dB is obtained from 6 GHz to 10 GHz.

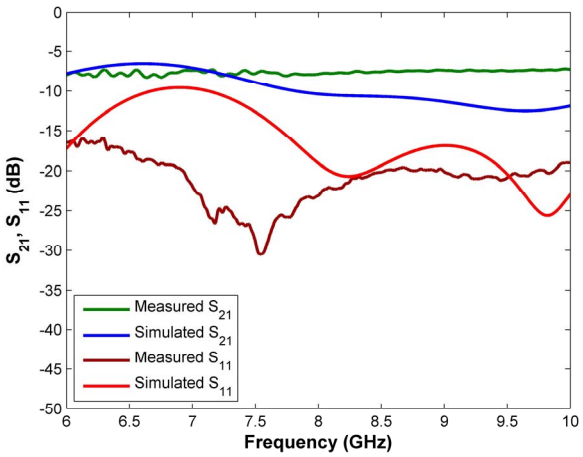

Fig. 12 S-parameter comparison between experimental and simulated results for R_s =55 Ω, forward current=70 µA.

Note that the initial goal of up to 6 dB attenuation has been achieved. However, measurements and simulations start to deviate for forward currents greater than 50 μA applied to each diode. This can be explained by the equivalent circuit (Fig. 6) which fails to represent the PIN diode's true behavior under these biasing conditions.

CONCLUSION

A HMSIW variable PIN diode attenuator operating in the frequency range between 6 GHz and 10 GHz is designed and experimentally verified. Surface-mount component integration is explored by adding four PIN diodes to the structure. By adjusting the level of the dc bias applied to the diodes, different levels of attenuation are achieved. After fine adjustment of the PIN diode's equivalent circuit, simulated and measured results present good agreement, and the initial goal of 6 dB attenuation is achieved as verified by measurements. Thus, these results show that the HMSIW PIN diode attenuator is operating properly. While the attenuation is not constant over the wide frequency band of 50 percent, the results demonstrate that the signal can be attenuated continuously over a range of up to 6 dB while maintaining a reflection coefficient of -10 dB or better.

REFERENCES

[1] M. Bozzi, L. Perregrini, K. Wu, and P. Arcioni, "Current and future research trends in substrate integrated waveguide technology," Radioengineering, vol. 18, no. 2, pp. 201–209, June 2009.

[2] F. Taringou, J. Bornemann, and K. Wu, "Broadband coplanar-waveguide and microstrip low-noise amplifier hybrid integrations for K-band substrate integrated waveguide applications on low-permittivity substrate," IET Microw. Antennas Propag., vol. 8, no. 2, pp. 99-103, Jan. 2014.

[3] F. Taringou, D. Dousset, J. Bornemann, and K. Wu, "Broadband CPW feed for millimeter-wave SIW-based antipodal linearly tapered slot antennas," IEEE Trans. Antennas Propagat., vol. 61, no. 4, pp. 1756-1762, Apr. 2013.

[4] B. Liu, W. Hong, Y.-Q. Wang, Q.-H. Lai, and K. Wu, "Half mode substrate integrated waveguide (HMSIW) 3-db coupler," IEEE Microw. Wireless Compon. Lett., vol. 17, no. 1, pp. 22–24, Jan. 2007.

[5] W. Hong, B. Liu, Y. Wang, Q. Lai, H. Tang, X.X. Yin, Y.D. Dong, Y. Zhang, and K. Wu, "Half mode substrate integrated waveguide: A new guided wave structure for microwave and millimeter wave application," in Proc. Joint 31st Int. Conf. Infrared Millimeter Waves and 14th Int. Conf. Teraherz Electronics, p. 219, Shanghai, China, Sep. 2006.

[6] Q. Lai, C. Fumeaux, W. Hong, and R. Vahldieck, "Characterization of the propagation properties of the half-mode substrate integrated waveguide," IEEE Trans. Microw. Theory Tech., vol. 57, no. 8, pp. 1996–2004, Aug. 2009.

[7] Z.-Y. Zhang and K. Wu, "Broadband half-mode substrate integrated waveguide (HMSIW) Wilkinson power divider," in IEEE MTT-S Int. Microw. Symp. Dig., pp. 879–882, Atlanta, USA, June 2008.

[8] Y.-Y. Huang, W. Woo, Y. Yoon, and C.-H. Lee, "Highly linear RF CMOS variable attenuators with adaptive body biasing," IEEE J. Solid-State Circuits, vol. 46, no. 5, pp. 1023–1033, May 2011.

[9] D.-S. Eom and H.-Y. Lee, "Broadband half mode substrate integrated waveguide attenuator in 7.29–14.90 GHz," ," IEEE Microw. Wireless Compon. Lett., vol. 25, no. 9, pp. 564-566, Sep. 2015.

[10] D.-S. Eom and H.-Y. Lee, "An X-band substrate integrated waveguide attenuator," Microw. Opt. Technol. Lett., vol. 56, no. 10, pp. 2446–2449, July 2014.

[11] K.-O. Sun, M. K. Choi, and D. van der Weide, "A PIN diode controlled variable attenuator using a 0-db branch-line coupler," IEEE Microw. Wireless Compon. Lett., vol. 15, no. 6, pp. 440–442, June 2005.

[12] Z. Kordiboroujeni and J. Bornemann, "Designing the width of substrate integrated waveguide structures," IEEE Microw. Wireless Compon. Lett., vol. 23, no. 10, pp. 518–520, Oct. 2013.

[13] F. Taringou, D. Dousset, J. Bornemann, and K. Wu, "Substrate-integrated waveguide transitions to planar transmission-line technologies," in IEEE MTT-S Int. Microw. Symp. Dig., pp. 1–3, Montreal, Canada, June 2012.

[14] D. Deslandes, "Design equations for tapered microstrip-to-substrate integrated waveguide transitions," in IEEE MTT-S Int. Microw. Symp. Dig., pp. 704–707, Anaheim, USA, May 2010.

[15] A. Strollo, "A new spice model of power p-i-n diode based on asymptotic wave-form evaluation," IEEE Trans. Power Electron., vol. 12, no. 1, pp. 12–20, Jan. 1997.

[16] S. Morel, H. Gamal and J. Chante, "A state variable modeling of the power pin diode using an explicit approximation of semiconductor device equations: A novel approach," IEEE Trans. Power Electron., vol. 9, no. 1, pp. 112–120, Jan. 1994.

[17] H. Garrab, B. Allard, H. Morel, K. Ammous. S. Ghedira, A. Amimi, K. Besbes, and J.-M. Guichon, "On the extraction of PIN diode design parameters for validation of integrated power converter design," IEEE Trans. Power Electron, vol. 20, no. 3, pp. 660–670, May 2005.

[18] F.L. Heutmaker, L.M. Fletcher, and J.E. Sohn, "Measurement of stray capacitance and inductance due to assembly variations in radio frequency circuit boards," in IEEE Princeton Section Sarnoff Symp. Dig., pp. 1–3, Princeton, USA, Apr. 1995.

[19] C. Poole and I. Darwazeh, Microwave Active Circuit Analysis and Design. Academic Press, 2015.

[20] D.M. Pozar, Microwave Engineering. John Wiley & Sons, 2009.